A Wide-Band, Circularly Polarized, Magnetodielectric Resonator Antenna

Amelia Buerkle, *Student Member, IEEE,* and Kamal Sarabandi, *Fellow, IEEE*

***Abstract*—Previously insurmountable challenges posed by stringent requirements of simultaneous compact size, high bandwidth, high to moderate efficiency, and circular polarization operation at UHF have been surpassed by a unique design employing layered magnetodielectric materials. To achieve percentage bandwidth values in excess of 50% for an antenna with a maximum dimension of 0.15λ three approaches for bandwidth enhancement are combined in a proper fashion. A volumetric source, as opposed to printed planar or wire sources, inherently provides higher bandwidth and is used as the fundamental radiating element of the antenna. The radiating structure is made up of layered magnetodielectric material with proper design of permittivity and permeability values forming a magnetodielectric resonator antenna (MDRA). Noting that miniaturization and wave impedance in the MDRA are, respectively, proportional to the square-root of the product and ratio of the permeability and permittivity, moderate values of permittivity and permeability are used to enhance the bandwidth while achieving considerable miniaturization. The third method for bandwidth enhancement is based on the integration of a resonant feed and many parasitic elements into the MDRA structure. Square symmetry of the MDRA is used to obtain circular polarization operation. A prototype small UHF antenna operating over 240–420 MHz with a linear dimension smaller than 0.15λ at the lowest frequency is fabricated and tested; the results are summarized in this paper.**

I. Introduction

SATELLITE communications is the most reliable and secure means of communication for civilian and military mobile platforms which provide global coverage. Operational satellite systems often require wide bandwidth or dual band operation. Circular polarization is also often required to remove the effects of polarization rotation due to propagation through the ionosphere. GPS systems, for example, which have low bandwidth requirements use microstrip patch antennas and, in some cases, quadrifilar helix antennas [1], [2]. In contrast, the civilian satellite system Globalstar is dual band, using 1.610–1.625 GHz for uplink and 2.4835–2.5 GHz for downlink [3]. Quadrifilar helix antennas are also used in this system [4]. Helical and spiral antennas inherently are able to produce circular polarization over a wide bandwidth [5]. However, such traveling wave type antennas must be large in dimension or comparable to the wavelength at the lowest frequency for proper operation. For mobile platforms, and specifically for airplanes and unmanned aerial vehicles, this may pose a limitation. This problem is exacerbated when operating at low UHF band where the wavelength is of the order of a meter. The challenges posed by a high bandwidth requirement in addition to possessing simultaneously compact size, high to moderate efficiency, and circular polarization have been met with a unique antenna design employing layered magnetodielectric materials.

The design begins with a dielectric resonator antenna (DRA) which, being a volumetric source, has inherently wider bandwidth than a linear or surface radiator [6]. In an effort to reduce the size, the DRA is composed of layers of magnetodielectric and dielectric materials, forming the MDRA. Finally, a previously developed method to improve the bandwidth of a DRA using a double resonant structure is used [7]. Extending this approach, parasitic elements are also included yielding a multiresonant design.

The design attributes are reviewed in Section II. The resonance frequency of the layered MDRA is approximated in Section III, the simulation setup is described in Section IV, and the fabrication details are given in Section V. Finally, measurement results are given in Section VI.

II. Design Development

A. Volumetric Radiator

The radiation power factor (RPF), developed by Wheeler, quantifies the ability of electrically small antennas to radiate [6]. The factor, which is inversely related to antenna Q, indicates the amount of real power radiated away from the antenna compared to the amount of reactive power stored in the antenna's near field. It is proportional to the ratio of effective antenna volume, which is related to its physical volume, to the volume of the radian sphere $(4\pi/3\,(\lambda/2\pi)^3)$. Volumetric sources, such as the MDRA, which more effectively fill the radian sphere have higher RPF and exhibit improved radiation capability and bandwidth. This is in contrast to linear and surface radiators which demonstrate considerably lower radiation bandwidth.

B. Magnetodielectric Materials

New materials are sought for enhanced miniaturization and simultaneously increased bandwidth. Here, we present the application of a recently developed magnetodielectric in the design of a MDRA. Antenna size is generally determined by the wavelength in the antenna material

$$\lambda_d = \frac{\lambda_o}{\sqrt{\mu_r \epsilon_r}} \tag{1}$$

where λ_o is the freespace wavelength and ϵ_r and μ_r are the relative permittivity and permeability, respectively. In the past, only high permittivity materials were available to decrease antenna

Manuscript received November 8, 2004; revised April 24, 2005. This work was supported by DARPA under Contract N000173-01-1-G910.

The authors are with the Radiation Laboratory, Electricla Engineering and Computer Science Department, University of Michigan, Ann Arbor, MI 48105 USA (e-mail: abuerkle@eecs.umich.edu).

Digital Object Identifier 10.1109/TAP.2005.858839

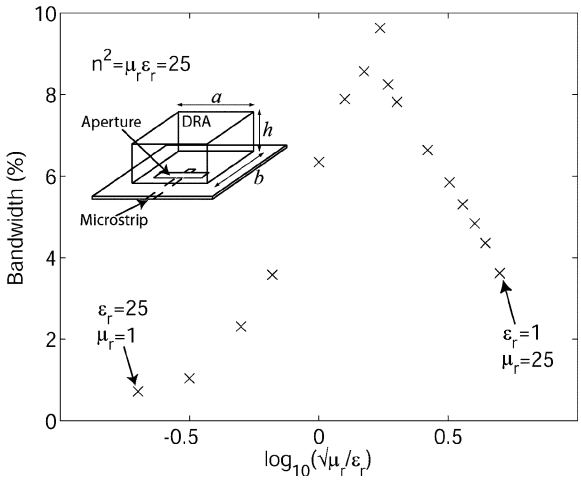

Fig. 1. Percent bandwidth versus the log of the MDRA intrinsic impedance. The slot-fed MDRA of dimensions $a \times b \times h$ is also shown.

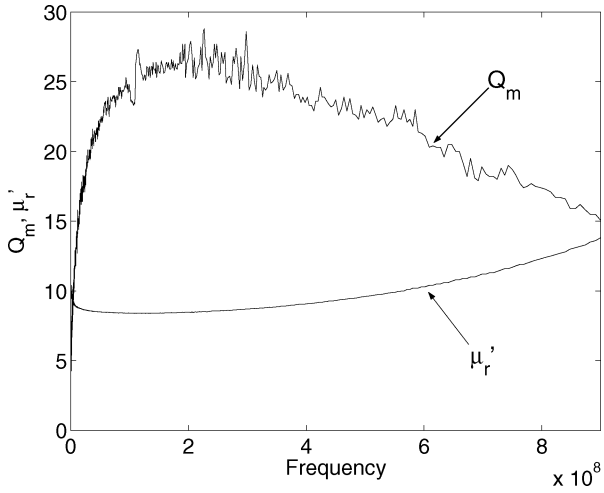

Fig. 2. Magnetic Q_m and relative permeability, μ_r', of the hexaferrite magnetodielectric versus frequency.

size; however, the use of such materials leads to increased energy storage in the antenna near field which in turn reduces the antenna bandwidth. Incorporating artificial materials with both μ_r and ϵ_r greater than unity can result in the same size antenna without the adverse effects of using high permittivity materials [8]. The lower contrast in wave impedance inside and outside the structure results in reduced entrapment of electromagnetic waves. Since energy storage is reduced, the ability of the structure to radiate power over a wider bandwidth is improved.

A study is carried out in simulation using the finite-difference time-domain (FDTD) method in order to investigate the effect of μ and ϵ on bandwidth [9]. Optimal values which maximize bandwidth for a particular slot-fed MDRA design are found. The results are given to provide qualitative evidence of the bandwidth improvement when both μ and ϵ are used. In each case, the intrinsic impedance ($\sqrt{\mu/\epsilon}$) is varied while the product of μ_r and ϵ_r is kept at 25, and the MDRA dimensions, $a = 0.2\lambda \times b = 0.2\lambda \times h = 0.13\lambda$, are held constant (see Fig. 1). The degree of matching varied as the permittivity and permeability were adjusted; modifications such as changing the slot length and position of the MDRA over the slot were made in order to achieve a -10 dB match. The fractional bandwidth of the MDRA resonance is plotted versus the log of the intrinsic impedance of the material ($\log_{10}\sqrt{\mu_r/\epsilon_r}$) in Fig. 1. It is observed that optimal bandwidth for this MDRA configuration is achieved when $\sqrt{\mu_r/\epsilon_r} = 1.74$, corresponding to $\mu_r = 8.62$ and $\epsilon_r = 2.9$. It is clearly demonstrated that, in general, by using a combination of both μ_r and ϵ_r the bandwidth can significantly be improved. In this case, a factor of improvement as large as 13 is observed. It is important to note that a high ratio of μ to ϵ may not be achievable even with a layered structure. In the fabricated design, as will be shown $\sqrt{\mu_r/\epsilon_r} \approx 0.8$.

If a similar design were attempted with dielectric materials, for the same resonant frequency and size, a higher permittivity material would be necessary. Using high permittivity materials alone makes the task of impedance matching and the use of multiresonant structures more complicated and sometimes impossible. Simulation results confirm narrower resonances and indicate poor coupling to the parasitic elements.

It is important to note that obtaining arbitrary ϵ and μ may not be possible physically. Until recently, low loss, high permeability, ferrite materials that operate over VHF-UFH bands were not available. Through a collaborative effort, supported by the DARPA metamaterials program, Trans-Tech, Inc., and the University of Michigan have developed a new class of these materials. In this design the magnetodielectric is an aligned Z-type hexaferrite ceramic. It is composed of barium hexaferrite blended with cobalt oxide and barium carbonate. The material's magnetic Q and the real part of the relative permeability are shown versus frequency in Fig. 2. Over the frequency range of interest, the magnetic loss tangent ($\tan\delta_m$) is approximately 0.04 but increases at higher frequencies; $\tan\delta_e$ is estimated to be five to ten times smaller than $\tan\delta_m$. The relative permittivity and permeability are approximately 16 and 8.5, respectively. Currently, the manufacturing process limits the hexaferrite layer thickness. Also, according to results in Fig. 1 a higher ratio of μ_r to ϵ_r than may be achieved with this material alone is desirable. As will be shown, an increased ratio can be achieved with a layered design of alternating hexaferrite and regular dielectric layers. Arranging the materials this way also improves the effective loss tangents.

C. Multiresonant Design for Increased Bandwidth

The technique used in [7] is shown to increase the impedance bandwidth of an antenna by using multiple resonant structures in the design. In particular, it combines a slot antenna and a DRA to effectively double the available bandwidth. With proper design it is observed that the resonance of the slot and that of the dielectric structure itself may be merged to achieve 100% bandwidth improvement over which the antenna polarization and radiation pattern are preserved. Using only dielectric materials fractional bandwidths on the order of 25% were demonstrated with moderate miniaturization.

One drawback of using a slot to feed the MDRA is back radiation; the slot dimensions necessary to merge the resonances may be large enough to allow nonnegligible radiation below the ground plane. In cases where isolation from the lower half-space is needed, a probe feed can be used. The probe feed approach

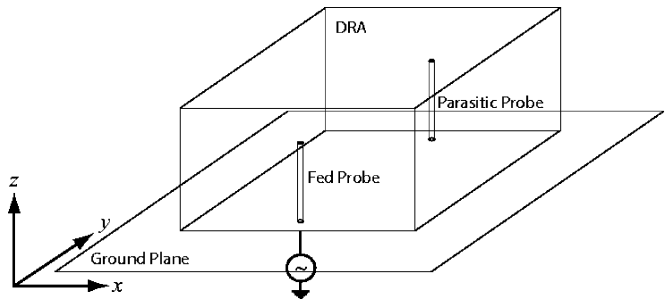

Fig. 3. Probe fed DRA with parasitic probe.

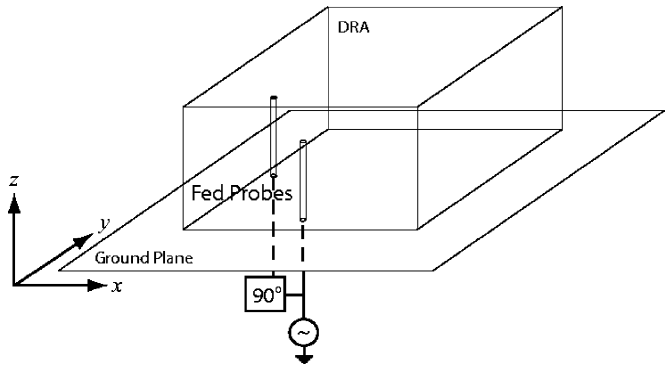

Fig. 4. Circularly polarized probe fed DRA.

also allows for easier implementation of a CP design. A minor drawback of using the probe feed is higher cross-pol levels in the H-plane of the MDRA (the x – z plane in Fig. 3). Loop feeds could instead be used to mitigate cross-pol radiation and allow for improved axial ratios; however, loop feeds are more difficult to fabricate than straight probes.

The concept of merging resonances to augment bandwidth can also be extended to include additional resonances from parasitic elements. If properly designed the parasitic element yields a third resonance at the proper frequency. For example, in the original design, an additional aperture was added next to the fed aperture. The two apertures are coupled through the electric field in the MDRA, each producing a distinct resonance; all three resonances would share the same linear polarization. The presence of the second aperture, however, exacerbates the problem of back radiation. Alternatively, a parasitic probe can be added on the other side of the MDRA, as shown in Fig. 3. In this design a parasitic probe is short circuited to the ground plane opposite from the fed probe. Additional parasitic probes can be added to achieve more resonances that would lead to increased bandwidth.

This multiresonance approach is used to design a circularly polarized antenna. A square MDRA is ideal for CP implementation because two orthogonal modes can be excited using two probes along adjacent walls, as shown in Fig. 4. At the MDRA resonance E_z has a null at the midpoint of the MDRA length in the y direction so the presence of the second probe should not affect the return loss at this frequency. At the probe resonance the effect of the second probe may be nonnegligible. However, based on the return loss simulated with and without the second CP probe the effect is not substantial.

III. First-Order MDRA Design

A simple procedure is outlined in order to provide a starting point for design. Effective medium theory is invoked to approximate the resonant frequency of the MDRA and probe. Since the layer thickness is small compared to the wavelength inside the MDRA an effective permittivity and permeability may be used to estimate the resonance frequency. Effective parameters are obtained by modeling the MDRA layers as series capacitors and inductors with values corresponding to their respective permittivity and permeability. These expressions should only apply to the z component of the parameters (ϵ_z, μ_z) as the transverse components ($\epsilon_{x,y}$, $\mu_{x,y}$) are not affected by the layered design. However, the resulting anisotropy is neglected in this approximation. This is acceptable for the dominant mode because the electric field is primarily in the $\hat{z}$ direction, perpendicular to the layers. In the case of equal thickness, alternating hexaferrite and dielectric layers

$$\mu_{r,\text{eff}} \approx \frac{\mu_{r1}+\mu_{r2}}{2} \approx 4.75 \quad \epsilon_{r,\text{eff}} \approx 2\Big(\frac{1}{\epsilon_{r1}}+\frac{1}{\epsilon_{r2}}\Big)^{-1} \approx 7 \tag{2}$$

where subscripts 1 and 2 refer, respectively, to the hexaferrite ($\epsilon_{r1}=16$, $\mu_{r1}=8.5$) and the dielectric ($\epsilon_{r2}=4.5$, $\mu_{r2}=1$) materials. Using these approximate values an effective index of refraction $n_{eff}=\sqrt{\mu_{r,\text{eff}}\epsilon_{r,\text{eff}}}\approx 5.8$ is achieved. The resonant frequency may be found using the familiar expressions given in [7] using the effective parameters derived above. The fundamental resonant frequency for the MDRA is chosen to be 264 MHz, slightly above the lower edge of the desired frequency band of 245 MHz. Solving the equations in [7] yields dimensions of 17.2 *cm* × 17.2 *cm* × 7.5 *cm*.

The first resonance of the feed and parasitic probes occurs at $\lambda_d/4$, where λ_d is the wavelength inside the MDRA. A length is selected such that the resonance occurs at a frequency adjacent to that of the MDRA.

IV. Simulation Results

The design is simulated using the FDTD method. In order to simplify the simulation model for the CP designs, the first probe is fed while the other fed probe is matched with a 50 Ω termination as it would be with the coupler. Therefore, the return loss reference plane is at the base of the fed probe rather than at the input to the coupler. Since the design is symmetric an identical result is obtained when the other input probe is fed. Isolation between the two antenna feeds is not investigated with FDTD simulation.

The return loss for the double resonant CP design, shown in Fig. 4, is given in Fig. 5. The MDRA resonance is around 265 MHz and the probe resonance is at 315.4 MHz. The size of the MDRA in this design is that obtained above, 17.2 cm × 17.2 cm × 7.5 cm, and the probe length is 4.3 cm.

The simulations were initiated with wire probes, as shown in Figs. 3 and 4. During initial measurements, it was observed that wider probes placed on the MDRA surface rather than wire probes inside result in better coupling to the MDRA. This type of probe also allows for easier setup and tuning. The simulated configuration was then updated to reflect the external probes.

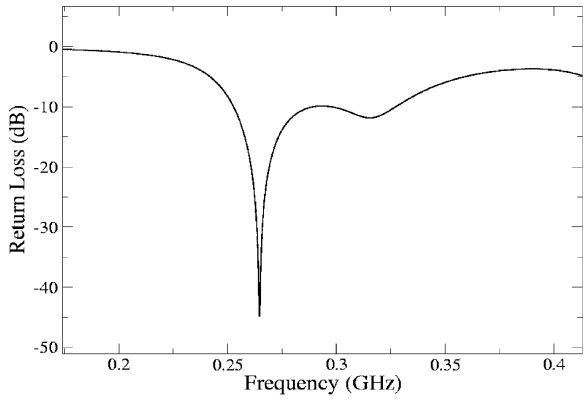

Fig. 5. Simulated return loss for the design shown in Fig. 4. Two fed, wire probes are used in this simulation; no parasitic probes are present.

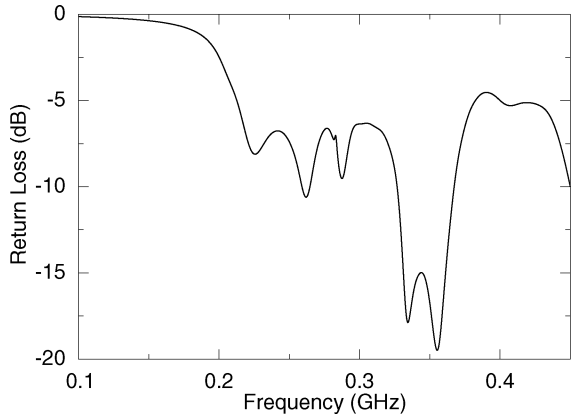

Fig. 6. Return loss simulated for the final design. Wider probes are used as in the antenna in the measurement section.

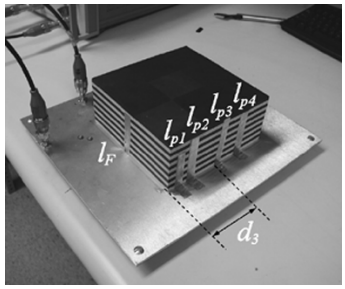

Fig. 7. Fabricated antenna in measurement setup with feed and parasitic elements.

Fig. 6 shows the simulation results for the return loss of the CP design shown in Fig. 7, which yields the measured results in Section VI. The resonance near 265 MHz is from the MDRA; additional resonances are from the fed and parasitic probes. The primary cause for disagreement between simulations and measurements is uncertainty in the isotropy and homogeneity of the hexaferrite antenna material. Since these properties have not yet been characterized they cannot be accounted for in simulation. The variation in the permeability within each hexaferrite tile is as large as $\mu_r = 8.5 \pm 0.5$; in addition, as seen in Fig. 2, both real and imaginary parts of μ vary over the band of interest. We use the FDTD method as a first order design tool. Primarily, it is used to obtain the size of the antenna necessary to operate at the desired band of frequencies (245–310 MHz). Following fabrication, further tuning was carried out in the lab.

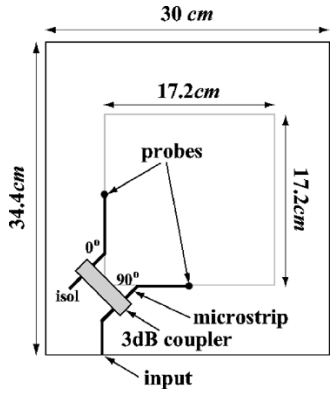

Fig. 8. Diagram of feed network using microstrip and a hybrid coupler.

TABLE I
PROBE DIMENSIONS AND LOCATIONS FOR THE DUAL LINEARLY POLARIZED AND CP DESIGNS

Probe	Width (cm)	Height (cm)	Location (cm)
l_F	1.2	6.9	8
l_{p1}	1.2	5.6	1.1
l_{p2}	1.4	7	3
l_{p3}	1.2	7.2	8
l_{p4}	1.4	7	11.5

V. FABRICATION DETAILS

As mentioned, the current fabrication procedure limits the hexaferrite thickness to roughly 0.5 cm. For this reason and also to improve the effective permeability to permittivity ratio of the MDRA, a layered design using regular dielectric layers alternated with hexaferrite layers is used. The dielectric layers used in the fabricated design are Roger's TMM4 and have relative permittivity of 4.5 with $\tan\delta_e < 0.002$.[1] The antenna is made of fourteen layers, each of which is 0.54 cm thick and 17.2 cm square. The hexaferrite layers are made up of smaller, 5 *cm* $\times$ 5 *cm* tiles that are glued together and machined to yield a smooth surfaced layer of uniform thickness. The total antenna height is about 7 cm. The fabricated antenna with feed and parasitic elements is shown in Fig. 7.

Two configurations using the same MDRA are built: a dual linearly polarized design and a CP design. The dual linearly polarized design consists of the two feed probes, eight parasitic elements (four for each fed probe), and the MDRA on a 30 cm square ground plane. This design is the same as that in the FDTD simulations. The CP design uses a 90° hybrid coupler to divide the input power to feed the two probes via microstrip as shown in Fig. 8. Coaxial feeds could also be used rather than microstrip. In this design the ground plane is approximately 30 cm by 34 cm. The probe dimensions and locations used in both designs are given in Table I; the probe designations correspond to those in Fig. 7. The location of the probe refers to the distance between

[1]Rogers Corporation, Rogers, CT. *http://www.rogers-corp.com*

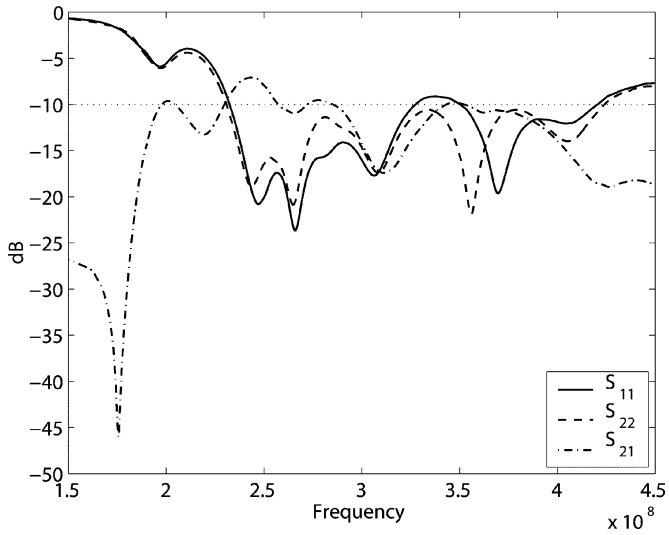

Fig. 9. Return loss and isolation of the dual linearly polarized design.

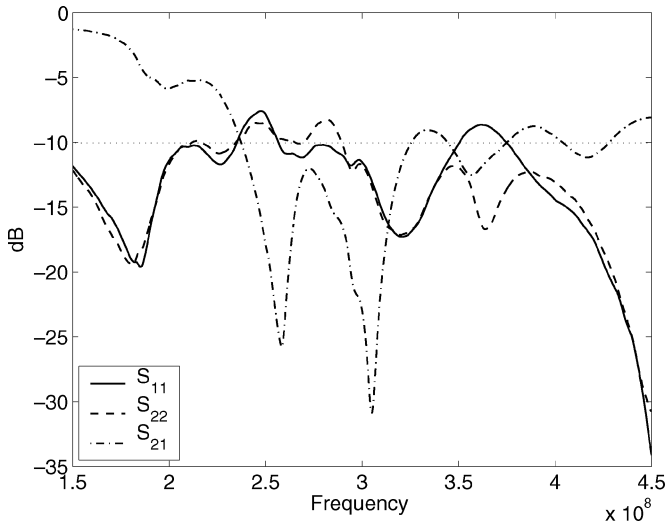

Fig. 10. Return loss and isolation measured with the CP feed network.

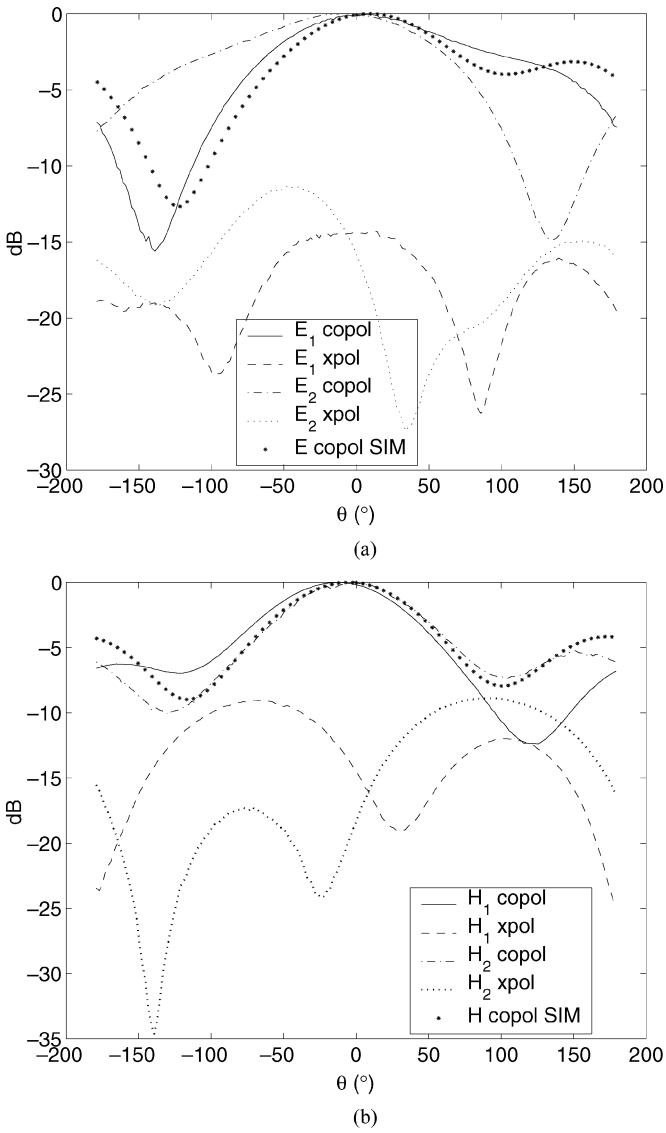

Fig. 11. E and H plane patterns at $f = 265$ MHz. (a) E plane pattern at $f = 265$ MHz. (b) H plane pattern at $f = 265$ MHz.

the left edge of the MDRA and the left edge of the probe; for example, in Fig. 7 the location of probe l_{p3} is indicated as d_3.

VI. Measurements

A. Return Loss and Isolation

The RF characteristics (return loss and port isolation) of the MDRA design shown in Fig. 7 are measured and reported in this section. The first set of measurements are carried out on the dual linearly polarized design; one port of the antenna is fed while the other is terminated with a matched load.

The return loss measured from each port is shown in Fig. 9. The measured impedance bandwidth covers a very wide bandwidth from 240–425 MHz. In order to ensure the input power is not absorbed in the matched load at the other port the isolation is measured as well. The result is also shown in Fig. 9. The isolation has a minimum of about -8 dB around 245 MHz, at the lower end of the operational bandwidth. This indicates that approximately 15% of the input power is lost in the matched termination. These results could be improved through further tuning, by compromising bandwidth for higher isolation.

The return loss is also measured with the CP feed network shown in Fig. 8. The second port of the network analyzer is connected to the isolated port of the coupler and is used to monitor the power reflected from the antenna ports. The result is shown in Fig. 10. The return loss is about -10 dB over the entire band; a minimum of -7.6 dB occurs at 248 MHz. The wideband matching is expected because power reflected from the antenna feeds goes to the isolated port of the coupler and shows up in S_{21}. The antenna operates when both S_{11} and S_{21} are below -10 dB; as in the previous measurement, this is above roughly 240 MHz.

B. Pattern and Gain Measurements

The patterns of the dual linearly polarized design are measured; the CP feed network is not used in pattern measurements. The E and H plane designations correspond to the MDRA planes. The E_1 and H_2 planes coincide as do the E_2 and H_1

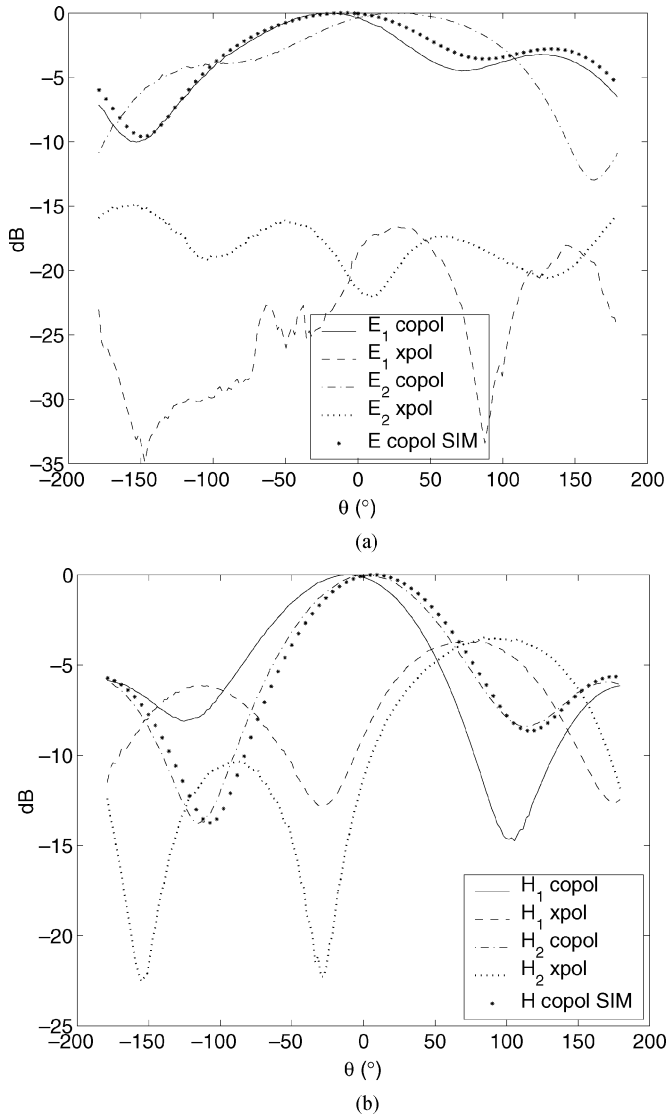

Fig. 12. E and H plane patterns at $f = 285$ MHz. (a) E plane pattern at $f = 285$ MHz. (b) H plane pattern at $f = 285$ MHz.

planes. The cross-pol level in the E plane may be effected by the presence of the cable during measurement. It is also noted that the anechoic chamber is designed for frequencies above 400 MHz. Therefore, these results may change with further measurement in an improved environment. The patterns measured at 246, 265, 285, and 310 MHz. Those at 265 and 285 MHz are shown in Figs. 11 and 12 with the simulated copol patterns. Patterns at the remaining frequencies are not shown because of space limitations. The symmetry in the design is evident in the patterns. The offset of the main beam is likely due to the presence of the parasitic probes.

The gain of the dual linearly polarized design is also measured. The results are shown in Table II. The size of the ground plane, in this case, is 50 cm square. The gain at higher frequencies is limited by the magnetic loss of the hexaferrite material which, as shown in Fig. 2, increases with increasing frequency. Considering the return loss and isolation between the two ports the expected antenna gain in the absence of dielectric and magnetic losses is about $+2$ dBi. This is about 3–4 dB higher than the measured gain values. Improving the magnetic loss can improve the antenna gain and current efforts are underway to reduce the magnetic loss tangent to values better than 10^{-2}.

TABLE II
GAIN MEASUREMENT RESULTS FOR THE DUAL LINEARLY POLARIZED DESIGN ON 50 CM GROUND PLANE (* 30 CM SQ)

f	G
250 MHz	-1 ± 1 dBi
259 MHz	-1.7 ± 1 dBi
280 MHz	-2 ± 1 dBi
310 MHz	-3 ± 1 dBi *

VII. CONCLUSION

The design presented in this paper combines three techniques to achieve percentage bandwidth values in excess of 50% for an antenna with a maximum dimension of 0.15λ. A volumetric MDRA structure, as opposed to printed planar or wire, is used. The MDRA is made up of layered magnetodielectric material with properly designed permittivity and permeability values. A resonant feed and parasitic elements are integrated into the MDRA design for enhanced bandwidth. Finally, the square symmetry of the MDRA is used in a CP design. Measurement results show the impedance percentage bandwidth is on the order of 58%. The design's primary limitations are in the cross-pol caused by the probe feeds and its efficiency. As noted, loop feeds could be used in a similar design with reduced cross-pol. Development of a lower loss hexaferrite is currently under consideration to improve the gain.

ACKNOWLEDGMENT

The authors would like to thank D. Cruickshank and J. Zheng from Trans-Tech for fabricating the antenna, and H. Mosallaei from the University of Michigan for his help with the FDTD simulation software.

REFERENCES

[1] W. S. T. Rowe, R. B. Waterhouse, and C. T. Huat, "Performance of a scannable linear array of hi-lo stacked patches," *Proc. Inst. Elect. Eng. Microwaves, Antennas, and Propagation*, vol. 150, no. 1, pp. 1–4, 2003.
[2] J. M. Tranquilla and S. R. Best, "A study of the quadrifilar helix antenna for global positioning system (GPS) applications," *IEEE Trans. Antennas Propag.*, vol. 38, no. 10, pp. 1545–1550, Oct. 1990.
[3] "Globalstar Retains Access to all of its Allocated U.S. Frequencies FCC Announcement Rules," Tech. Rep., Jun. 2004. [Online]. Available: www.globalstarusa.com
[4] D. F. Filipovic, M. A. Tassoudji, and E. Ozaki, "A coupled-segment quadrifilar helical antenna," in *Proc. IEEE MTT-S Symp. Technologies Wireless Applications Dig.*, Feb. 1997, pp. 43–46.
[5] C. Balanis, *Antenna Theory*. New York: Wiley, 1997.
[6] H. A. Wheeler, "Fundamental limits of small antennas," in *Proc. IRE.*, Dec. 1947.
[7] A. Buerkle, K. Sarabandi, and H. Mosallaei, "Compact slot and dielectric resonator antenna with dual-resonance, broadband characteristics," IEEE Trans. Antennas Propag., vol. 53, no. 3, pp. 1020–1027, Mar. 2004, to be published.
[8] H. Mosallaei and K. Sarabandi, "Magnetodielectrics in electromagnetics: Concepts and applications," *IEEE Trans. Antennas Propag.*, vol. 52, no. 6, pp. 1558–1567, Jun. 2004.
[9] H. Mosallaei, "Complex layered materials and periodic electromagnetic band-gap structures: concepts, characterizations, and applications," Ph.D. dissertation, Univ. California, Los Angeles, 2001.

Amelia Buerkle (S'03) received the B.Sc. degree in electrical engineering from The Cooper Union, New York, in May 2002 and the M.S. degree in electrical engineering from the University of Michigan, Ann Arbor, in April 2004, where she is currently working towards the Ph.D. degree in the Radiation Laboratory.

Her current research interests include dielectric resonator antennas and metamaterials.

Ms. Buerkle is a recipient of a National Science Foundation (NSF) Graduate Research Fellowship.

Kamal Sarabandi (S'87–M'90–SM'92–F'00) received the B.S. degree in electrical engineering from Sharif University of Technology, Tehran, Iran, in 1980, the M.S. degree in electrical engineering/mathematics, and the Ph.D. degree in electrical engineering from The University of Michigan-Ann Arbor, in 1986 and 1989, respectively.

He is Director of the Radiation Laboratory and a Professor in the Department of Electrical Engineering and Computer Science, The University of Michigan-Ann Arbor. He has 20 years of experience with wave propagation in random media, communication channel modeling, microwave sensors, and radar systems and is leading a large research group consisting of four research scientists, ten Ph.D. students, and two M.S. students. Over the past ten years he has graduated 20 Ph.D. students. He has served as the Principal Investigator on many projects sponsored by NASA, JPL, ARO, ONR, ARL, NSF, DARPA, and numerous industries. He has published many book chapters and more than 125 papers in refereed journals on electromagnetic scattering, random media modeling, wave propagation, antennas, microwave measurement techniques, radar calibration, inverse scattering problems, and microwave sensors. He has also had more than 300 papers and invited presentations in many national and international conferences and symposia on similar subjects. His research areas of interest include microwave and millimeter-wave radar remote sensing, electromagnetic wave propagation, and antenna miniaturization.

Dr. Sarabandi is a Member of the International Scientific Radio Union (URSI) Commission F and D, and The Electromagnetic Academy. He was the recipient of the Henry Russel Award from the Regent of The University of Michigan (the highest honor the University of Michigan bestows on a faculty member at the assistant or associate level). He was also a recipient of a 1996 EECS Department Teaching Excellence Award. In 1999, he received a GAAC Distinguished Lecturer Award from the German Federal Ministry for Education, Science, and Technology given to about ten individuals worldwide in all areas of engineering, science, medicine, and law. In 2004, he received a College of Engineering Research Excellence Award. In 2005, he received two prestigious awards, namely, the IEEE Geoscience and Remote Sensing Distinguished Achievement Award and the University of Michigan Faculty Recognition Award. In the past several years, joint papers presented by his students at a number of international symposia have received top student prize paper awards (IEEE AP'95,'97,'00,'01,'03, IEEE IGARSS'99,'02, IEEE IMS'01, URSI' 04,'05). He is a Vice President of the IEEE Geoscience and Remote Sensing Society (GRSS), and a Member of IEEE Technical Activities Board Awards Committee. He is an Associate Editor of the IEEE TRANSACTIONS ON ANTENNAS AND PROPAGATION and the IEEE SENSORS JOURNAL. He is listed in *American Men & Women of Science*, *Who's Who in America*, and *Who's Who in Science and Engineering*.